

In vivo time-resolved spectroscopy of the human bronchial early cancer autofluorescence

Pascal Uehlinger
Tanja Gabrecht
Thomas Glanzmann
Jean-Pierre Ballini

Swiss Federal Institute of Technology in Lausanne (EPFL)
Institute of Chemical Sciences and Engineering
Station 6
CH-1015 Lausanne, Switzerland

Alexandre Radu

Centre Hospitalier Universitaire Vaudois Lausanne
Ear, Nose, and Throat Department
Hospices-CHUV
CH-1011 Lausanne, Switzerland

Snezana Andrejevic

Centre Hospitalier Universitaire Vaudois Lausanne
Institute of Pathology
Rue du Bugnon 27
Hospices-CHUV
CH-1011 Lausanne, Switzerland

Philippe Monnier

Centre Hospitalier Universitaire Vaudois Lausanne
Ear, Nose, and Throat Department
Hospices-CHUV
CH-1011 Lausanne, Switzerland

Georges Wagnières

Swiss Federal Institute of Technology in Lausanne (EPFL)
Institute of Chemical Sciences and Engineering
Station 6
CH-1015 Lausanne, Switzerland

1 Introduction

Lung cancer is the most common cancer in the world, and it is responsible for more deaths in the developed countries than any tumors of other organs.¹ Five-year survival rates after diagnosis fluctuate between 8% and 12% in Europe^{2,3} and are less than 15% in North America.⁴ One cause of this low survival rate is the fact that the disease is often already in an advanced stage when symptoms occur. However, screening studies in high-risk patients with low-dose computer tomography have shown that early detection of the disease can dramatically increase the survival rate.^{5,6} White-light bronchoscopy is the diagnostic method of choice to detect and biopsy endobronchial cancer. However, only about 30% of the carcinoma *in situ* (CIS) and two thirds of the microinvasive carcinomas are visible under standard white-light endoscopy.⁷

Address all correspondence to: Georges Wagnières, Swiss Federal Institute of Technology (EPFL), Station 6, Building CH, 1015 Lausanne, Switzerland. Tel. +41 21 693 3120; Fax +41 21 693 3626; E-mail: georges.wagnieres@epfl.ch.

Abstract. Time-resolved measurements of tissue autofluorescence (AF) excited at 405 nm were carried out with an optical-fiber-based spectrometer in the bronchi of 11 patients. The objectives consisted of assessing the lifetime as a new tumor/normal (T/N) tissue contrast parameter and trying to explain the origin of the contrasts observed when using AF-based cancer detection imaging systems. No significant change in the AF lifetimes was found. AF bronchoscopy performed in parallel with an imaging device revealed both intensity and spectral contrasts. Our results suggest that the spectral contrast might be due to an enhanced blood concentration just below the epithelial layers of the lesion. The intensity contrast probably results from the thickening of the epithelium in the lesions. The absence of T/N lifetime contrast indicates that the quenching is not at the origin of the fluorescence intensity and spectral contrasts. These lifetimes (6.9 ns, 2.0 ns, and 0.2 ns) were consistent for all the examined sites. The fact that these lifetimes are the same for different emission domains ranging between 430 and 680 nm indicates that there is probably only one dominant fluorophore involved. The measured lifetimes suggest that this fluorophore is elastin. © 2009 Society of Photo-Optical Instrumentation Engineers. [DOI: 10.1117/1.3088100]

Keywords: autofluorescence (AF); bronchial cancer detection; fluorescence lifetime spectroscopy; imaging; neoplasia; dysplasia; specificity.

Paper 08329R received Sep. 12, 2008; revised manuscript received Jan. 6, 2009; accepted for publication Jan. 13, 2009; published online Mar. 19, 2009.

Therefore, approaches using fluorescence from exogenous and endogenous fluorophores have been undertaken in our and other institutions⁸⁻¹² in order to improve the sensitivity and specificity of standard white-light endoscopy. Above all, the approach of using fluorescence of the endogenous fluorophores, i.e., the autofluorescence (AF), is very appealing, as it does not require the administration of a contrast agent. Autofluorescence bronchoscopy (AFB) is based on the visualization of the spectral and intensity contrasts of the bronchial AF between the healthy mucosa and preneoplasia or neoplasia. This application has proven to be highly sensitive to early, noninvasive preneoplastic and microinvasive neoplastic lesions that may remain occult with conventional white-light bronchoscopy.¹³⁻¹⁷ Commercially available AFB systems mostly utilize blue-violet light for the AF excitation and detect the AF intensity contrast in the green part of the spectrum.^{12,16,18-22} Optimal contrast can be achieved with excitation wavelengths around 405 nm (Ref. 23). However, al-

though the sensitivity of AFB for preneoplasia and microinvasive neoplasia is high, its specificity remains limited.^{13,15,16} In addition, the mechanisms that are at the origin of the contrasts between healthy mucosa and lesions are not clearly identified at the present time.

The steady-state approach employed by the AFB systems integrates the emitted AF signal over time, ignoring the dynamics of the AF decay and losing an additional dimension of information. Time-resolved spectrofluorometric measurements capture the decay of the AF intensity in time and thus provide further information about the characteristics of specific fluorophores and their microenvironment. Indeed, time-resolved fluorescence spectroscopy for tumor detection is of interest for numerous reasons: (1) The AF from biological tissues stems from several endogenous fluorophores with overlapping spectra. If the relative concentration of these fluorophores varies, a lifetime contrast can be expected. (2) Quantitative measurements of the AF intensity are difficult to perform during endoscopy, whereas fluorescence lifetime measurements are independent of the signal intensity. (3) The fluorescence lifetime of several endogenous fluorophores is sensitive to the physicochemical properties of their microenvironment and may thus be an indicator of biochemical variations occurring already in the early phases of preneoplastic changes.

Indeed, time-resolved AF spectroscopy and imaging have been previously investigated for diagnosis in the colon,²⁴ skin,^{25,26} breast,²⁷ head and neck,²⁸ as well as the urinary bladder,²⁹ among others. Consequently, the decision was made to study the AF lifetime in order to determine whether the AF decay parameters could be used as a novel means of establishing a contrast between healthy bronchial mucosa and preneoplastic or microinvasive neoplastic lesions [in the following, referred to as (pre-)neoplasia]. An instrument enabling *in vivo* point measurements on the bronchial mucous membrane during endoscopy³⁰ was developed for this purpose. This instrumentation was used in parallel with the steady-state AF imaging device built by our group,¹¹ and this combination enabled the localization of suspicious sites by the imaging device and, subsequently, the point-measurements of the fluorescence lifetimes at these locations.

The purpose of the time-resolved fluorescence measurements was not merely to answer the question of whether the AF lifetime might be a parameter providing a reliable contrast between healthy mucosa and (pre-)neoplasia, but also to shed new light on the query regarding the origin of the AF contrast observed with imaging systems.^{23,31,32} Several hypotheses are generally evoked to explain the spectral contrasts observed between endobronchial (pre-)neoplasia and their healthy counterpart: (1) A decrease in concentration of the fluorophores in the (pre-)neoplastic lesion. (2) A quenching of the fluorescence by a change of the physicochemical environment in the lesion, e.g., the pH and/or pO₂ values. (3) An architectural effect, i.e., a thickening of the epithelium in the lesion due to abnormal cell proliferation. Since most of the AF seems to originate from the submucosa,³² this could induce a decrease in AF intensity measured on the surface of the mucosa. (4) An increased concentration of light absorbers such as hemoglobin. Time-resolved fluorescence measurements can reveal whether the fluorescence quenching plays a significant role. Last, it should be noted that these AF lifetime measure-

ments must be carried out *in vivo* due to some of the endogenous fluorophores such as reduced nicotinamide adenine dinucleotide (NADH) and flavins being known to exhibit various spectral properties depending on their redox state or to photobleach rapidly.^{33,34} In addition, blood content also changes in resected specimens.^{31,32} It is worth noting that most studies aimed at characterizing biological tissues by AF lifetime have been conducted on *ex vivo* samples,^{25,27,28} and reports on *in vivo* studies are scarce.²⁴

2 Materials and Methods

2.1 Time-Resolved Fluorescence Measurements

The instrumentation for the time-resolved spectroscopic fluorescence measurements has been described in detail elsewhere.³⁰ Briefly, the excitation light pulses (typical pulse duration about 500 ps, repetition ratio 10 Hz) of a nitrogen laser-pumped dye laser emitting at 405 nm (MSG 803TD, LTB GmbH, Berlin, Germany) were injected into a 550- μm -core-diam optical fiber using a UV-coated lens and a dichroic long-pass filter (cutoff wavelength 450 nm, 45-deg arrangement). The fiber could be easily inserted into the working channels of conventional flexible bronchoscopes, and its flat distal cut-end was applied in direct gentle contact with the lesions or normal respiratory mucous membrane. This geometry, combined with the limited penetration depth of violet (405 nm) light, defines a probed volume of typically 0.1 mm³. The laser light delivered by the fiber excited the mucosa AF that was collected by the same fiber. The fluorescence signal was transmitted through the dichroic filter and injected into a spectrograph (250IS, Chromex, Albuquerque, New Mexico). An additional 430-nm long-pass filter positioned in front of the spectrograph removed the remaining backscattered excitation light, and an entire time-resolved spectrum could thus be acquired by means of a streak camera (C4334, Hamamatsu Photonics K.K., Hamamatsu City, Japan) that was operated in the analog mode in the 20-ns time window. The spectral resolution was approximately 15 nm, and the temporal resolution was 280 ps. Each individual measurement consisted of the integration of 150 acquisitions (see the following below). The entire setup was installed on a trolley for transport to the procedure room.

Measurements performed on a reference sample (quartz cuvette for optical spectroscopy containing 3 ml of rhodamine 6G, 10 μM in water) were carried out prior to the endoscopic analysis in order to compensate for the variations of the excitation light intensities, optical alignment, and detector performance. The AF intensities were subsequently normalized by the signal intensity of this reference and expressed in relative units (r.u.). This procedure allowed a comparison of the fluorescence intensities from different patients. This reference sample was also used to validate our fluorescence lifetime measurement system and data analysis procedure. As reported in detail by Glanzmann et al.,³⁰ the lifetime measured on this reference sample was compatible with the literature. In addition, a mono-exponential decay was obtained with an excellent reproducibility (variations on the order of 2%) on this sample. Our group also performed measurements on reference samples containing a mixture of rhodamines. The individual fluorescence lifetimes could be identified with a higher than 20% precision using our fluorescence lifetime measurement

system and data analysis procedure. Last, it should be noted that similar measurements were performed on various luminescence standards exhibiting luminescence lifetimes ranging between 0.175 and 3700 ns. The excellent agreement between these measurements and the literature indicate that the response of our instrument is reliable within this time range.³⁰ However, it is worth noting here that the shortest measured lifetimes, the component τ_1 defined below, were inferior to the width of the excitation laser pulse and were thus likely to be biased. For this reason, these shortest lifetimes were not taken into account in the comparison, presented here, of the results from the spectrometric and imaging studies.

2.2 The AF Imaging Device

The AF imaging device has been described in detail elsewhere.¹² Briefly, it consisted of a filtered endoscopic light source and a filtered 3 CCD endoscopic camera (both from Richard Wolf GmbH, Knittlingen, Germany). The light source contained a 300-W xenon lamp and was equipped with a flip-flop filter holder containing (1) a custom-made blue-violet bandpass filter (390 nm to 460 nm) for AF excitation, and (2) a grid for conventional white-light (WL) endoscopy. The light was led to the endoscope optics via a liquid light guide, and the endoscopic image (WL and AF) was detected by the 3 CCD camera. A 490-nm long-pass filter in the camera objective rejected all blue-violet excitation light. When the light source was employed in the AF mode, i.e., emitting blue-violet light, the blue color channel of the camera was suppressed. Thus, the AF images obtained with this system contained only the green (500 nm to 590 nm) and red (>600 nm) color information. The camera head could be clipped to conventional rigid bronchoscopes or to a dedicated bronchofiberscope. The bronchoscopic images were displayed on a video monitor (Sony, Japan) and recorded with a video recorder to enable their subsequent analysis by a computer after digitization. This procedure provided quantitative information regarding the green and red AF intensities. Due to the spectral and intensity changes mentioned earlier, healthy bronchial mucosa appeared greenish (AF negative), whereas (pre-)neoplastic lesions presented a brown-reddish color (AF positive).

2.3 In Vivo Measurements

Eleven high-risk lung cancer patients undergoing conventional white-light bronchoscopy (WLB) and diagnostic AFB were included in the present study. A total of 14 bronchoscopies, referred to in the following as *a case*, were performed on these patients. The inclusion criteria were positive sputum cytology, positive resection margins following previous lung cancer surgery, and routine follow-up bronchoscopy. Both WLB and AFB were performed with the AF bronchofiberscope described earlier, and the locations of AF-positive as well as AF-negative, i.e., healthy, sites were identified. For the time-resolved measurements, the optical fiber of the spectrofluorometer was inserted into the working channel of the bronchoscope and placed in gentle contact with the mucous membrane under visual control. The acquisition time was approximately 15 s. For each measurement, two acquisitions were performed on a single spot without moving the fiber, with the aim of verifying whether the contact with the mucosa

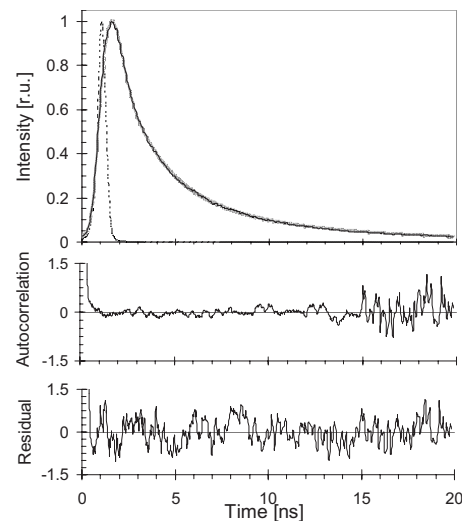


Fig. 1 A 3-exponential least-square deconvolution fit of an AF decay in the range of 510 to 550 nm. Upper panel: The dashed line depicts the excitation pulse at 405 nm, whereas the black solid line and the gray patterned line represent the decay data and fit function, respectively. The lower figures display the autocorrelation function as well as the residuals.

had been established through the entire duration of the measurement. The two acquisitions were considered void if they were not identical. Whenever possible, measurements were repeated on the same site after slightly displacing the fiber in order to account for intrapatient variations due to local heterogeneities of the bronchial mucosa. Measurements were performed on all lesions identified with the AFB imaging system. Additional measurements on the healthy mucosa were carried out at various locations in the bronchial tree so as to assess the anatomy-dependent intra- and interpatient variations. More precisely, measurements were performed on the carina, the walls of the main bronchi, as well as on the spurs of the upper- and lower-lobe bronchi. Biopsies were taken with WLB or AFB on suspect sites, and the presence or absence of (pre-)neoplasia was evaluated by subsequent histopathological analysis. The whole procedure was recorded on video. In histopathologic analysis, the specimens were classified into the following three categories: (1) reactive change including basal cell hyperplasia and squamous metaplasia; (2) preneoplasia without invasion of the basement membrane, including mild, moderate, and severe dysplasia, as well as CIS; and (3) neoplasia, including microinvasive carcinoma and invasive squamous cell carcinoma.

2.4 Lifetime Analysis

The fluorescence decays were analyzed using the Marquardt-Levenberg iterative nonlinear least-squares reconvolution fitting algorithm, assuming an *a priori* multiexponential decay (Software HPD-TA-Fit 2.1.3, Hamamatsu Photonics Germany GmbH, Herrsching, Germany). The signal-to-noise ratio of the obtained decays enabled a fit with up to three exponentials. The resulting curves of the weighted residuals as well as the autocorrelation of the residuals versus channel number are shown for graphical assessment of the goodness of fit (Fig. 1). Good fits should yield randomly distributed residuals about

zero. The presence of any pattern in the distribution of either the residuals or the autocorrelation function is an indication that the model used is inadequate to describe the data. Bad fits provide low-frequency periodicity in an autocorrelation plot that can be easily detected.³⁵ The AF decays were analyzed for two wavelength ranges 510 nm to 550 nm and 600 nm to 640 nm, corresponding to the green and red spectral detection ranges, respectively, of the AFB imaging device. Figure 1 shows the AF decay between 510 nm and 550 nm on healthy bronchial mucosa together with the excitation pulse and the curves of both the residuals and the autocorrelation function. As demonstrated in the figure, the fits with three decay parameters gave rise to curves of both the residuals and the autocorrelation function. The slight modulation of both curves as well as a weak odd-even effect was due to the response characteristics of the streak camera. As can be seen on the left part of the autocorrelation curve, the range of the fit could not be extended all the way to the beginning of the decay profile. This was probably the result of a slight difference in pulse and decay profile due to the nonlinearity of the so-called cross talk of the streak camera. Nevertheless, the fitted results were very stable, and the 3-exponential fits gave rise to considerably enhanced residual curves as opposed to their 2-exponential counterparts. The 4-exponential fits, on the other hand, led to unstable results, and no improvement of the residuals was obtained.

The relative photonic weight of each lifetime was calculated using the expression $\alpha_i * \tau_i / (\sum_i \alpha_i * \tau_i)$, where τ_i is the AF lifetime, and α_i is a preexponential factor. In order to characterize the speed of fluorescence decay with a single parameter, the *10%-decay-time*, designating the time period during which the fluorescence decreased from its maximum value to 10% of its intensity, was introduced. This approach enabled, in typical conditions, a quantification of the differences in decay time at the center of the decay curve, since the time-window of the streak camera was 20 ns, as can be seen in Fig. 1.

2.5 AF Image Analysis

For each case, one WL and one AF image per spectroscopically measured and biopsied site were digitized in the 24-bit RGB color scheme. The average intensity of the red (R) and green (G) pixels of the biopsied lesion as well as of the presumably healthy surrounding mucosa (reference) were computed together with their standard deviations. These values were used to compute (1) the intensity ratios in the green and the red color channels {ratio $R'_{\text{green}(\text{red})}$ between the green (red) intensities on the lesion and the corresponding intensities on the reference area [Eq. (1)]} and (2) the normalized red-to-green color ratio R'_{norm} between the lesion and the reference area [Eq. (2)]:

$$R'_{\text{red}} = \frac{R_{\text{lesion}}}{R_{\text{reference}}} \text{ and } R'_{\text{green}} = \frac{G_{\text{lesion}}}{G_{\text{reference}}}, \quad (1)$$

$$R'_{\text{norm}} = \frac{R'_{\text{red}}}{R'_{\text{green}}} = \left(\frac{R_{\text{lesion}}}{R_{\text{reference}}} \right) : \left(\frac{G_{\text{lesion}}}{G_{\text{reference}}} \right). \quad (2)$$

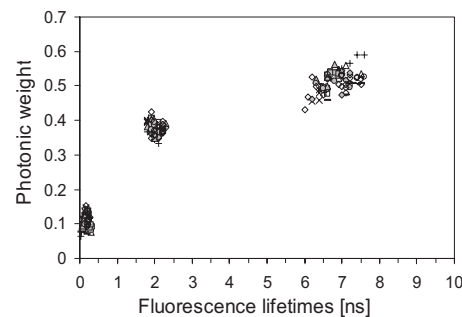


Fig. 2 Lifetimes and normalized photonic weights of the AF decays on the healthy bronchial mucosa of 11 patients between 510 and 550 nm at 405-nm excitation. (Each patient corresponds to one symbol.)

Equations (1) and (2) show the computation of the red and green intensity ratios R' [Eq. (1)] and of the normalized color ratio R'_{norm} , where R_{lesion} (G_{lesion}) and $R_{\text{reference}}$ ($G_{\text{reference}}$) represent the red (green) pixel intensities calculated from the lesion and the reference area, respectively.

3 Results

3.1 Intra- and Interpatient Variations of the Lifetime Parameters

The inpatient variations of the AF lifetime due to mucosa heterogeneities and changes in the anatomical structure were assessed from 14 cases, including 11 patients as described in Sec. 2. Figure 2 compares the calculated AF lifetimes measured from healthy mucosa at various locations of the tracheo-bronchial tree during the 14 exams against their normalized relative photonic weight. All lifetimes extracted from decays measured during a single exam are indicated with the same sign. This renders it possible to compare the intra- and the interpatient variation.

The mean values of three AF lifetimes, τ_1 , τ_2 , and τ_3 , were 0.17 ± 0.07 ns, 2.02 ± 0.13 ns, and 6.84 ± 0.39 ns, respectively, with variations on the order of 39%, 6.4%, and 5.7%, respectively. The corresponding variations for the photonic weights were 17.9%, 4.0%, and 5.9%, respectively. Approximately 50% of the fluorescence stems from the long lifetime τ_3 , about 40% from the intermediate lifetime τ_2 , and close to 10% from the short lifetime τ_1 .

The mean inpatient variations in the fluorescence lifetimes were on the order of 17.3% (range 6.5% to 35.4%) for the shortest lifetime τ_1 and approximately 4% (range 1.5% to 7%) for the longer lifetimes τ_2 and τ_3 . The corresponding inpatient variations of the photonic weights ranged from 3.5% to 7.7%. Although the measurements of the individual patients were somewhat grouped, the interpatient variations were no more pronounced than their inpatient counterparts. As already stated, the inpatient variations result partially from mucosa heterogeneities, but also from changes in the AF of the tissues related to the anatomical structure of the bronchi.

The variations in AF lifetime due to mucosa heterogeneities are illustrated by the open triangles and open diamonds in Fig. 2, representing seven and five measurements, respectively, conducted at neighboring spots on the healthy carina of

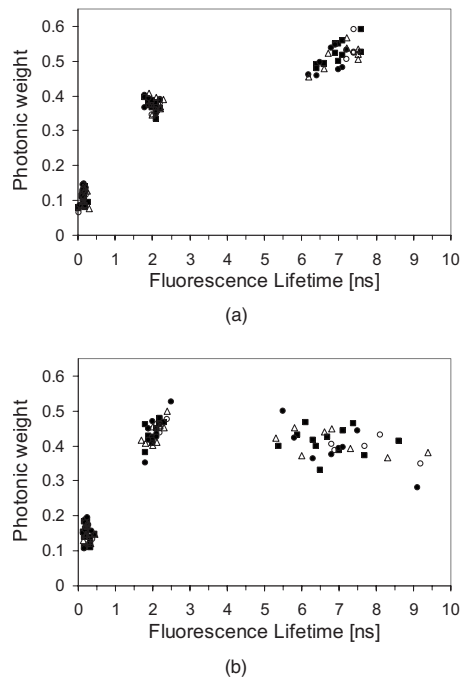


Fig. 3 Photonic weights versus AF lifetimes measured on healthy mucosa on (1) the main carina (squares); (2) superior spurs (open circles); (3) inferior spurs (circles); and (4) the walls of the stem bronchi (triangles). Figure 3(a) shows the results for the green spectral region (510 nm to 550 nm), whereas Fig. 3(b) displays those for the red spectral region (600 nm to 640 nm).

two patients. These inpatient variations were on the order of 35%, 3.8%, and 3.9% for the lifetimes τ_1 , τ_2 , and τ_3 , respectively.

Figures 3(a) and 3(b) show the distribution of the AF lifetimes from healthy bronchial mucosa for the green [510 to 550 nm³; Fig. 3(a)] and red [600 to 640 nm; Fig. 3(b)] spectral regions, respectively. The figures represent data from a subgroup of eight patients for which data in both spectral regions were available. The mean AF lifetimes computed for the fluorescence decays in the red spectral region (τ_1 : 0.25 ± 0.08 ns, τ_2 : 2.06 ± 0.20 ns, τ_3 : 6.98 ± 1.08 ns) were relatively similar to those in the green spectral region (τ_1 : 0.15 ± 0.06 ns, τ_2 : 2.04 ± 0.19 ns, τ_3 : 6.97 ± 0.41 ns). [95% confidence interval (CI) and *p*-value of the "red-green" lifetimes populations differences: τ_1 : (0.065 to 0.135; $p < 0.05$), τ_2 : (-0.076 to 0.116, $p > 0.05$), τ_3 : (-0.392 to 0.411, $p > 0.05$)] In addition, the figures show the correlation between the AF lifetime and the anatomic localization of the measured site. No dependence on the location in the bronchi of either the AF lifetimes or the relative photonic weight was observed in either of the spectral regions. Moreover, the changes in the AF lifetimes originating from measurements performed at various locations in the bronchi were comparable to the AF lifetime variations due to the heterogeneity of the mucosa response, as shown in Fig. 2.

Due to the similarity of the principal AF lifetimes in the green and the red spectral regions, all data presented in the following paragraphs refer exclusively to the green spectral region. This approach could also be justified by the fact that the decrease in intensity observed in spatially resolved

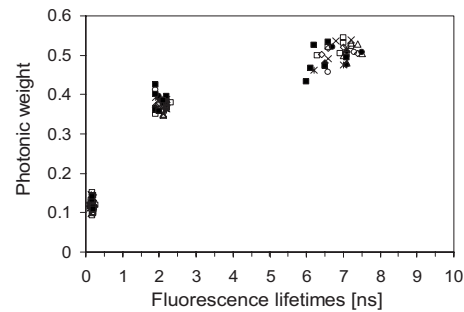


Fig. 4 Lifetimes and normalized photonic weights (wavelength range 500 nm to 590 nm) of the autofluorescence decays on three severe dysplasia, two microinvasive carcinoma, and healthy mucosa measured in five cases. Each symbol corresponds to one measurement. Solid symbols depict measurements on TP lesions, whereas open symbols refer to measurements on surrounding healthy mucosa.

spectrofluorometry^{8,23,32} and imaging^{11,12,16} was most important in the green spectral region and was thus the principal cause for the AF contrast.

It is worth noting that although the lifetimes did not depend on the localization of the measurement spot within the bronchial tree, the fluorescence intensities did. At wavelengths ranging from 510 nm to 550 nm, the fluorescence intensities measured on the spurs of the upper and lower bronchi were twofold lower (relative intensities $I_{rel} = 42.6 \pm 15.8$ and 33.6 ± 19.6 , respectively) than those measured on the carina ($I_{rel} = 81 \pm 37.2$) and on the wall of the main bronchi ($I_{rel} = 79.5 \pm 38.8$); data not shown.

3.2 AF Lifetimes of (Pre-)Neoplastic Lesions

A total number of eight lesions were detected by AF bronchoscopy in 5 of the 11 patients. All lesions were invisible with conventional white-light bronchoscopy. Histopathologic analysis of the biopsies taken from the lesions confirmed five (pre-)neoplasia (three severe dysplasia and two microinvasive carcinoma) and three reactive changes (squamous metaplasia). The former are here referred to as true positives (TP) and the latter as false positives (FP). The photonic weights of the various AF lifetimes detected in the green spectral region for the TP lesions (solid symbols) and the surrounding healthy mucosa (open symbols) are presented in Fig. 4.

Figure 4 does not demonstrate a systematic difference in the photonic weight or AF lifetime computed for healthy mucosa and (pre-)neoplasia, respectively. This was confirmed by statistical analysis giving the 95% CI and the *p*-values for the three lifetimes as follows: τ_1 (95% CI: -0.0285 to 0.085, $p > 0.05$), τ_2 (95% CI: -0.0282 to 0.1482, $p > 0.05$), and τ_3 (95% CI: -0.0209 to 0.5609, $p > 0.034$). The results from the AF lifetime measurements were compared to the color aspect and intensity ratios computed from the AFB images. For four of the five (pre-)neoplasias (two severe dysplasia and two microinvasive carcinoma), a complete set of data, including AFB and WLB images, as well as AF lifetime measurements for both the lesion and its surrounding healthy mucosa, was available for analysis. Figures 5(a) and 5(b) display the AF lifetimes in the green spectral region versus the intensity ratios R' and R'_{norm} . Although the ratios computed from the AFB images clearly show evidence of a spectral and intensity

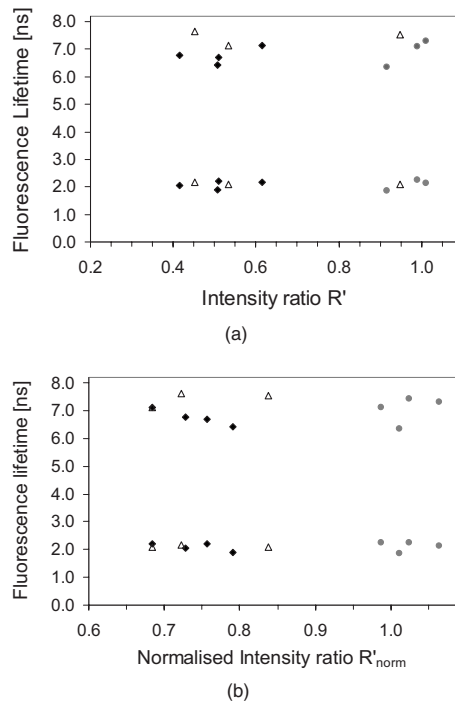


Fig. 5 AF lifetimes (wavelength range 500 nm to 590 nm) τ_2 and τ_3 of four true positive (TP) lesions and three false positive (FP) lesions found in two patients versus the intensity ratios as computed from the AFB images. (a) AF lifetimes measured on the lesion versus the green (R' , diamonds) intensity ratios between TP (solid symbols) and FP (open symbols) lesions and healthy mucosa (gray circles). (b) AF lifetimes measured on the lesion versus the normalized R'_{norm} intensity ratio for TP (solid squares) and FP (open squares) lesions. The gray circles depict the AF lifetime measured on healthy mucosa versus the R'_{norm} for the same sites.

contrast between the lesions and their surrounding healthy mucosa, no difference in the AF lifetimes measured on the respective sites could be observed.

As mentioned earlier, it is worth noting here that the shortest measured lifetimes τ_1 were inferior to the width of the excitation laser pulse and were thus likely to be biased. For this reason, the shortest lifetimes were not taken into account in the comparison of the results from the spectrometric and imaging study.

Figure 6 displays the relative peak AF intensities measured between 510 nm and 550 nm as functions of the 10% decay

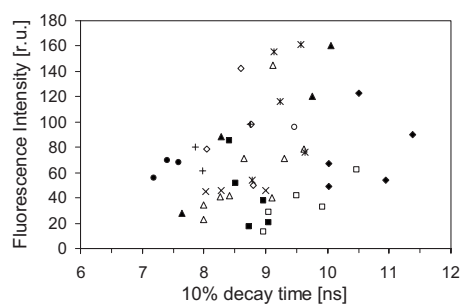


Fig. 6 The relative peak fluorescence intensity between 510 nm and 560 nm versus the 10% decay time measured on healthy bronchial mucosa in 11 patients. (Each symbol corresponds to one patient.)

time for 47 measurements performed on the healthy mucosa of 11 patients. Each symbol depicts values measured at various locations in the same patient. As described earlier, the 10% decay time permitted a characterization of the speed of the AF decay by a single parameter.

The relative inter- and inpatient variations in the AF intensities were 56% and 40%, respectively. Furthermore, the inter- and inpatient variations of the 10% decay time were on the order of 10% and 5.4% (range 7 ns to 11.5 ns), respectively, and thus markedly smaller than the intensity variations. The measurements of the relative fluorescence intensity with an optical fiber were extremely difficult to perform on small spurs due to the patient's heartbeats and the often complex geometries in the bronchi. It was thus first believed that the analysis conditions were at the origin of the significant AF intensity variations. However, the measurements conducted at the easily accessible carina of the same patient—shown in Fig. 2 (open triangles)—demonstrated that the local heterogeneities in the bronchial wall in terms of intensities and decay parameters were as high as the inpatient variation resulting from measurements on other, less accessible locations in the bronchi. This contradicted the idea that poor measurement conditions were responsible for the fluctuations observed. The 10% decay time and AF intensities from the measurements on the carina are also displayed as open triangles in Fig. 6.

Since the variations in the 10% decay time were small and very poorly correlated with the intensity, the intensity variations could not be attributed to fluorescence quenching, but were rather believed to be due to changes in the concentrations of fluorochromes and/or absorber or to variations in the structure of the bronchial wall.

4 Discussion

The present work describes an investigation of the potential of time-resolved *in vivo* spectrofluorometry for discriminating preneoplastic or microinvasive neoplastic lesions and healthy mucosa in the bronchi. To our knowledge, this study is the first to explore the AF lifetime parameters of human bronchial mucosa *in vivo*. Clinical studies performed by other groups in the colon and on oral mucosa have shown a potential of AF lifetimes to allow discrimination between tissues of different histopathologies. In contrast to these preliminary results, our time-resolved measurements revealed no differences in the decay parameters obtained from healthy bronchial mucosa and preneoplastic or neoplastic lesions. Although these results were based on only a limited number of patients, the data suggested that the difference in the lifetime parameters—if present—should be small in comparison to the inter- and inpatient variations of the AF on healthy mucosa.

There were two main reasons for the limited number of lesions: first, the measurements with the optical fiber were difficult to perform in accordance with clinical routine, thus limiting the total number of patients included in the study; second, the aim of the study was to investigate the properties of flat, (pre-)neoplastic lesions that remain invisible with conventional WL bronchoscopy. This type of lesion is typically found in about 13% of the investigated patient population.³⁶ Nevertheless, despite the intra- and interpatient variations, the data from the entirety of the measurements were consistent. It was thus very unlikely that an increased amount of data would

change the results and interpretations of the study.

The analysis of the AF variations in the mucosa permitted conclusions to be drawn on the origin of the contrasts observed with the AFB imaging system. Three types of variations could be distinguished: (1) inpatient variations due to local heterogeneities in the bronchial mucosa, (2) inpatient differences due to anatomical changes, and (3) interpatient variations. Among these, the mucosa heterogeneities accounted for most of the changes with regard to the lifetime decay. When comparing the variations in the AF intensity measured with the spectrofluorometer's fiber in contact with the mucosa to those observed in the AFB images, i.e., those obtained at distances of several millimeters, it turned out that the heterogeneity of the AF intensity was considerably less pronounced on the images. Consequently, the heterogeneities that were at the origin of the variations observed with the spectrofluorometer must be confined to the surface. Furthermore, the investigations of the AF intensities measured with the spectrofluorometer displayed differences of one order of magnitude, while the variations of the decay time were less than 10%. Consequently, a fluorescence quenching could not be the main reason for these intensity and spectral variations on the healthy mucosa. Rather, a local thickening of the poorly fluorescing epithelium resulting in a decrease of the detected AF could be evoked as a hypothesis. Additionally, the subepithelial layers of the bronchial wall (lamina propria and submucosa) contained nonhomogeneously distributed, absorbing tissue structures, including blood vessels and smooth muscle strings, which could have contributed to local variations in the detected AF intensities. Due to the different fluorescence collection geometries, these irregularities could be averaged out in the case of the distance measurements with the imaging AFB system. Their impact on the fiber-based contact measurements was, on the other hand, much more important.

As already stated in the introduction, most AFB imaging systems are based on the detection of the intensity contrast observed in the green part of the spectrum between (pre-)neoplastic lesions and their surrounding healthy mucosa. Although these intensity contrasts could not, due to the reasons explained earlier, be determined with our time-resolved spectrofluorometer, the analysis of the images obtained with our AFB imaging system clearly demonstrated an intensity and spectral contrast of the AF between all lesions that had also been measured with our spectrofluorometer and their surrounding healthy mucosa [Fig. 5(a)]. This was in agreement with results obtained from fiber-based contact measurements with a space-resolved spectrofluorometer on formalin-fixed histopathologic samples, confirming the presence of the intensity contrast between (pre-)neoplastic lesions and their surrounding healthy mucosa.¹⁹ Such an intensity contrast is believed to be the result of a local thickening of the epithelial layer in (pre-)neoplastic lesions, shielding the AF from deeper-lying tissue layers.

Our results also provide interesting information about the main fluorochromes responsible for the bronchial mucosa AF. Among the fluorophores reported to be found in human tissues, flavins, NADH, elastin, and porphyrins are likely to be excited at 405 nm (Ref. 16). The emitted AF in the blue part of the spectrum (430 nm to 500 nm) could be due to NADH and elastin, whereas the AF in the green-yellow part

(500 nm to 600 nm) could result from flavins and elastin, and the yellow-red part (>600 nm) could originate from elastin, flavins, and possibly porphyrins. *In vitro* measurements have been reported in the literature that attribute rather long fluorescence lifetimes to elastin (0.5 ns, 2.6 ns, and 7.8 ns), short lifetimes to NADH when bound to proteins (0.37 ns, 1.1 ns, and 2.4 ns), and intermediate lifetimes to oxidized flavin adenine dinucleotide (FAD) (0.16 ns, 2.25 ns, and 4.6 ns).³⁷⁻³⁹

Most studies aiming at employing the AF lifetime for diagnostic purposes focus on the excitation and detection of NADH and FAD fluorescence. Indeed, both molecules show characteristic changes in their AF signature—excitation wavelength, quantum yield, emission spectrum, and lifetime—when their redox state is changed, i.e., when being involved in metabolic processes. Moreover, it has been shown that the relative concentrations of NADH and FAD, as well as their metabolic variants in certain biological tissues, can be used as a diagnostic tool for neoplasia and cancer.^{40,41}

Nevertheless, the calculated AF lifetimes presented in Figs. 2–4 match the reported lifetimes of elastin quite well. This is in agreement with results recently published by Thiberville et al.⁴² regarding an examination of the structure of the human bronchial wall *in vivo* using a fibered confocal fluorescence microscope. The authors concluded that the AF signal in the proximal bronchi originates mainly from elastin situated in the subepithelial layers. Moreover, a fibered fluorescing structure was observed, which became disorganized in the presence of (pre-)neoplastic lesions and was even absent in invasive squamous cell carcinoma. These results correspond to observations of Kobayashi et al.⁴³ who reported on a strong correlation between the detected AF intensity and the density of elastin in the examined areas on human bronchus samples excited with light at around 400 nm. Indeed, recent genetic studies have shown an increased interstitial transcription of matrix metalloproteinase-12 (MMP-12), which is the macrophage elastase, in pulmonary non-small-cell squamous cell carcinoma. Interestingly, these transcripts were not increased in the adjacent healthy mucosa.

The principal degradation products of elastin by MMPs are amino acids such as glycine, alanin, and valin, among others.⁴⁴ The excitation wavelengths for these amino acids are all inferior to 295 nm (Ref. 39), and these molecules will thus not contribute to the AF signal obtained with our spectrofluorometer or the AFB system. Consequently, it is very likely that the degradation of the elastin network in (pre-)neoplastic lesions induces changes in the AF intensity and spectral shape, as observed with the AFB systems, while leaving the AF lifetimes measured with our systems unchanged. However, the destruction of the elastin network alone cannot explain the spectral and intensity AF contrasts observed with the AFB imaging devices.

In summary, the present study has shown that the AF lifetime excited at 405 nm does not have the potential to discriminate (pre-)neoplastic lesions from healthy bronchial mucosa. More precisely, the presence of the AF contrasts between lesions and healthy mucosa observed in the spectral domain cannot be linked to induce measurable changes of the AF lifetime. Nevertheless, our results have provided new insights into the mechanisms that are at the origin of the AF

spectral and intensity contrasts. Indeed, according to the measurements, fluorescence quenching in the upper layer of the bronchial mucosa plays only a minor role, if any, in the generation of the AF contrasts. However, the AF from the elastin network in the submucosa provides the major fluorescence signal with an excitation wavelength of around 405 nm. It is thus likely that pathologic changes in the elastin network contribute to the AF contrasts observed with the AFB imaging systems.

Acknowledgments

We gratefully acknowledge support from the Swiss National Fund for Scientific Research, Grants Nos. 205 320-116556, and from the Fonds de Service and Fonds de Perfectionnement of the ENT, Head and Neck Surgery Department, at the CHUV Hospital.

References

1. A. Jemal, R. Siegel, E. Ward, T. Murray, J. Xu, and M. J. Thun, "Cancer statistics, 2007," *Ca-Cancer J. Clin.* **57**(1), 43–66 (2007).
2. I. Guessous, J. Cornuz, and F. Paccaud, "Lung cancer screening: current situation and perspective," *Swiss Med. Wkly* **137**(21–22), 304–311 (2007).
3. F. Levi, F. Lucchini, C. La Vecchia, E. Negri, and F. Levi, "Trends in mortality from major cancers in the European Union, including acceding countries, in 2004," *Cancer (N.Y.)* **101**(1), 2843–2850 (2004).
4. C. I. Henschke, "Early lung cancer action project: overall design and findings from baseline screening," *Cancer (N.Y.)* **89**(11 Suppl.), 2474–2482 (2000).
5. C. I. Henschke, D. F. Yankelevitz, D. M. Libby, M. W. Pasmantier, J. P. Smith, and O. S. Miettinen, "Survival of patients with stage I lung cancer detected on CT screening," *N. Engl. J. Med.* **355**(17), 1763–1771 (2006).
6. S. Diederich, "Lung cancer screening: status in 2007 [Screening des Lungenkarzinoms: Stand 2007]," *Der Radiologe* **48**(1), 39–44 (2008).
7. S. Lam and H. D. Becker, "Future diagnostic procedures," *Chest Surg. Clin. N. Am.* **6**(2), 363–380 (1996).
8. M. Tercelj, H. Zeng, M. Petek, T. Rott, and B. Palcic, "Acquisition of fluorescence and reflectance spectra during routine bronchoscopy examinations using the ClearVu Elite device: pilot study," *Lung Cancer* **50**(1), 35–42 (2005).
9. G. Wagnieres, W. Star, and B. Wilson, "In vivo fluorescence spectroscopy and imaging for oncological applications," *Photochem. Photobiol.* **68**(5), 603–632 (1998).
10. S. Lam, T. Kennedy, and M. Unger, "Localization of bronchial intraepithelial neoplastic lesions by fluorescence bronchoscopy," *Chest* **113**(3), 696–702 (1998).
11. D. Goujon, M. Zellweger, A. Radu, P. Grosjean, B.-C. Weber, H. van den Bergh, P. Monnier, and G. Wagnieres, "In vivo autofluorescence imaging of early cancers in the human tracheobronchial tree with a spectrally optimized system," *J. Biomed. Opt.* **8**(1), 17–25 (2003).
12. T. Gabrecht, T. Glanzmann, L. Freitag, B. C. Weber, H. Van Den Bergh, and G. Wagnieres, "Optimized autofluorescence bronchoscopy using additional backscattered red light," *J. Biomed. Opt.* **12**(6), 064016 (2007).
13. K. Häußinger, F. Stanzel, M. Kohlhäufel, H. Becker, F. Herth, A. Kreuzer, B. Schmidt, J. Strausz, S. Cavaliere, K.-M. Müller, R.-M. Huber, U. Pichlmeier, and C. T. Bolliger, "Autofluorescence bronchoscopy with white light bronchoscopy compared with white light bronchoscopy alone for the detection of precancerous lesions: a European randomized controlled multicenter trial," *Thorax* **60**(6), 496–503 (2005).
14. N. Ikeda, H. Honda, A. Hayashi, J. Usuda, Y. Kato, M. Tsuboi, T. Ohira, T. Hirano, H. Kato, H. Serizawa, and Y. Aoki, "Early detection of bronchial lesions using newly developed videoendoscopy-based autofluorescence bronchoscopy," *Lung Cancer* **52**(1), 21–27 (2006).
15. P. N. Chhajed, K. Shibuya, H. Hoshino, M. Chiyo, K. Yasufuku, K. Hiroshima, and T. Fujisawa, "A comparison of video and autofluorescence bronchoscopy in patients at high risk of lung cancer," *Eur. Respir. J.* **25**(6), 951–955 (2005).
16. G. Wagnieres, A. McWilliams, and S. Lam, "Lung cancer imaging with fluorescence endoscopy," in *Handbook of Biomedical Fluorescence*, M.-A. Mycek and B. W. Pogue, Eds., pp. 361–396, Marcel Dekker, Inc., New York (2003).
17. T. Gabrecht, A. Radu, M. Zellweger, B. Lovisa, D. Goujon, P. Grosjean, H. van den Bergh, P. Monnier, and G. Wagnieres, "Autofluorescence bronchoscopy: clinical experience with an optimized system in head and neck cancer patients," *Med. Laser Appl.* **22**(3), 185–192 (2007).
18. P. Lee, H. A. Brokx, P. E. Postmus, and T. G. Sutedja, "Dual digital video-autofluorescence imaging for detection of pre-neoplastic lesions," *Lung Cancer* **58**(1), 44–49 (2007).
19. T. Gabrecht, S. Andrejevic-Blant, and G. Wagnieres, "Blue-violet excited autofluorescence spectroscopy and imaging of normal and cancerous human bronchial tissue after formalin fixation," *Photochem. Photobiol.* **83**(2), 450–458 (2007).
20. L. Fuso, G. Pagliari, V. Boniello, A. Trove, F. Varone, A. Longobardi, S. Basso, and L. Trodella, "Autofluorescence bronchoscopy to identify pre-cancerous bronchial lesions," *Monaldi Arch. Chest Dis.* **63**(3), 124–128 (2005).
21. A. Ernst, D. Feller-Kopman, and W. Lunn, "Autofluorescence bronchoscopy and endobronchial ultrasound: a practical review," *Ann. Thorac. Surg.* **80**(6), 2395–2401 (2005).
22. M. Chiyo, K. Shibuya, H. Hoshino, K. Yasufuku, Y. Sekine, T. Iizasa, T. Fujisawa, and K. Hiroshima, "Effective detection of bronchial pre-invasive lesions by a new autofluorescence imaging bronchovideoscope system," *Lung Cancer* **48**(3), 307–313 (2005).
23. M. Zellweger, P. Grosjean, D. Goujon, P. Monnier, H. van den Bergh, and G. Wagnieres, "In vivo autofluorescence spectroscopy of human bronchial tissue to optimize the detection and imaging of early cancers," *J. Biomed. Opt.* **6**(1), 41–51 (2001).
24. M. A. Mycek, K. T. Schomacker, and N. S. Nishioka, "Colonic polyp differentiation using time-resolved autofluorescence spectroscopy," *Gastrointest. Endosc.* **48**(4), 390–394 (1998).
25. P. A. A. De Beule, C. Dunsby, N. P. Galletly, G. W. Stamp, A. C. Chu, U. Anand, P. Anand, C. D. Benham, A. Naylor, and P. M. W. French, "A hyperspectral fluorescence lifetime probe for skin cancer diagnosis," *Rev. Sci. Instrum.* **78**(12), 123101 (2007).
26. N. P. Galletly, J. McGinty, C. Dunsby, F. Teixeira, J. Requejo-Isidro, I. Munro, D. S. Elson, M. A. Neil, A. C. Chu, P. M. French, and G. W. Stamp, "Fluorescence lifetime imaging distinguishes basal cell carcinoma from surrounding uninvolved skin," *Br. J. Dermatol.* **159**(1), 152–161 (2008).
27. P. J. Tadrous, J. Siegel, P. M. French, S. Shousha, E. N. Lalani, and G. W. Stamp, "Fluorescence lifetime imaging of unstained tissues: early results in human breast cancer," *J. Pathol.* **199**(3), 309–317 (2003).
28. H. M. Chen, C. P. Chiang, C. You, T. C. Hsiao, and C. Y. Wang, "Time-resolved autofluorescence spectroscopy for classifying normal and premalignant oral tissues," *Lasers Surg. Med.* **37**(1), 37–45 (2005).
29. J. Mizeret, G. Wagnieres, T. Stepinac, and H. Van Den Bergh, "Endoscopic tissue characterization by frequency-domain fluorescence lifetime imaging (FD-FLIM)," *Lasers Med. Sci.* **12**(3), 209–217 (1997).
30. T. Glanzmann, J. P. Ballini, H. Van Den Bergh, and G. Wagnieres, "Time-resolved spectrofluorometer for clinical tissue characterization during endoscopy," *Rev. Sci. Instrum.* **70**(10), 4067–4077 (1999).
31. J. Qu, C. MacAulay, S. Lam, and B. Palcic, "Laser-induced fluorescence spectroscopy at endoscopy: tissue optics, Monte Carlo modeling, and in vivo measurements," *Opt. Eng. (Bellingham)* **34**(11), 3334–3343 (1995).
32. J. Qu, C. MacAulay, S. Lam, and B. Palcic, "Optical properties of normal and carcinomatous bronchial tissue," *Appl. Opt.* **33**(31), 7397–7405 (1994).
33. K. T. Schomacker, J. K. Frisoli, C. C. Compton, T. J. Flotte, J. M. Richter, N. S. Nishioka, and T. F. Deutsch, "Ultraviolet laser-induced fluorescence of colonic tissue: basic biology and diagnostic potential," *Lasers Surg. Med.* **12**, 63–78 (1992).
34. F. W. D. Rost, "Autofluorescence in human and animal tissues," in *Fluorescence Microscopy II* F. W. D. Rost, Ed., pp. 1–15, Cambridge University Press, Cambridge, UK (1995).
35. D. F. Eaton, "Recommended methods for fluorescence decay analysis," *Pure Appl. Chem.* **62**(8), 1631–1648 (1990).
36. S. J. Stoeckli, R. Zimmermann, and S. Schmid, "Role of routine

- panendoscopy in cancer of the upper aerodigestive tract," *Otolaryngol.-Head Neck Surg.* **124**(2), 208–212 (2001).
37. M. Wakita, G. Nishimura, and M. Tamura, "Some characteristics of the fluorescence lifetime of reduced pyridine nucleotides in isolated mitochondria, isolated hepatocytes, and perfused rat liver *in situ*," *J. Biochem. (Tokyo)* **118**(6), 1151–1160 (1995).
 38. L. Pfeifer, K. Schmalzigaug, R. Paul, J. Lichey, K. Kemnitz, and F. Fink, "Time-resolved autofluorescence measurements for the differentiation of lung-tissue states," *Proc. SPIE* **2627**, 129–135 (1995).
 39. R. Richards-Kortum and E. Sevick-Muraca, "Quantitative optical spectroscopy for tissue diagnosis," *Annu. Rev. Phys. Chem.* **47**(1), 555–606 (1996).
 40. M. C. Skala, K. M. Riching, A. Gendron-Fitzpatrick, J. Eickhoff, K. W. Eliceiri, J. G. White, and N. Ramanujam, "*In vivo* multiphoton microscopy of NADH and FAD redox states, fluorescence lifetimes, and cellular morphology in precancerous epithelia," *Proc. Natl. Acad. Sci. U.S.A.* **104**(49), 19494–19499 (2007).
 41. J. D. Pitts, R. D. Sloboda, K. H. Dragnev, E. Dmitrovsky, and M. A. Mycek, "Autofluorescence characteristics of immortalized and carcinogen-transformed human bronchial epithelial cells," *J. Biomed. Opt.* **6**(1), 31–40 (2001).
 42. L. Thiberville, S. Moreno-Swirc, T. Vercauteren, E. Peltier, C. Cave, and G. Bourg Heckly, "*In vivo* imaging of the bronchial wall microstructure using fibered confocal fluorescence microscopy," *Am. J. Respir. Crit. Care Med.* **175**(1), 22–31 (2007).
 43. M. Kobayashi, K. Shibuya, H. Hoshino, and T. Fujisawa, "Spectroscopic analysis of the autofluorescence from human bronchus using an ultraviolet laser diode," *J. Biomed. Opt.* **7**(4), 603–608 (2002).
 44. R. P. Mecham, T. J. Broekelmann, C. J. Fliszar, S. D. Shapiro, H. G. Welgus, and R. M. Senior, "Elastin degradation by matrix metalloproteinases. Cleavage site specificity and mechanisms of elastolysis," *J. Biol. Chem.* **272**(29), 18071–18076 (1997).